Published in final edited form as:
Mamm Genome. 2004 March ; 15(3): 151–161.

New intragenic deletions in the *Phex* gene clarify X-linked hypophosphatemia-related abnormalities in mice

Bettina Lorenz-Depiereux[1,*], **Victoria E. Guido**[2,*], **Kenneth R. Johnson**[2], **Qing Yin Zheng**[2], **Leona H. Gagnon**[2], **Joiel D. Bauschatz**[2], **Muriel T. Davisson**[2], **Linda L. Washburn**[2], **Leah Rae Donahue**[2], **Tim M. Strom**[1], and **Eva M. Eicher**[2]

[1] Institute of Human Genetics, GSF National Research Center, Ingolstädter Landstr. 1,85764 München-Neuherberg, Germany

[2] The Jackson Laboratory, 600 Main Street, Bar Harbor, Maina 04609, USA

Abstract

X-linked hypophosphatemic rickets (XLH) in humans is caused by mutations in the PHEX gene. Previously, three mutations in the mouse *Phex* gene have been reported: $Phex^{Hyp}$, *Gy*, and $Phex^{Ska1}$. Here we report analysis of two new spontaneous mutations in the mouse *Phex* gene, $Phex^{Hyp\text{-}2J}$ and $Phex^{Hyp\text{-}Duk}$. $Phex^{Hyp\text{-}2J}$ and $Phex^{Hyp\text{-}Duk}$ involve intragenic deletions of at least 7.3 kb containing exon 15, and 30 kb containing exons 13 and 14, respectively. Both mutations cause similar phenotypes in males, including shortened hind legs and tail, a shortened square trunk, hypophosphatemia, hypocalcemia, and rachitic bone disease. In addition, mice carrying the $Phex^{Hyp\text{-}Duk}$ mutation exhibit background-dependent variable expression of deafness, circling behavior, and cranial dysmorphology, demonstrating the influence of modifying genes on *Phex*-related phenotypes. Cochlear cross-sections from $Phex^{Hyp\text{-}2J}$/Y and $Phex^{Hyp\text{-}Duk}$/Y males reveal a thickening of the temporal bone surrounding the cochlea with the presence of a precipitate in the scala tympani. Evidence of the degeneration of the organ of Corti and spiral ganglion also are present in the hearing-impaired $Phex^{Hyp\text{-}Duk}$/Y mice, but not in the normal-hearing $Phex^{Hyp\text{-}2J}$/Y mice. Analysis of the phenotypes noted in $Phex^{Hyp\text{-}Duk}$/Y an $Phex^{Hyp\text{-}2J}$/Y males, together with those noted in $Phex^{Ska1}$/Y and $Phex^{Hyp}$/Y males, now allow XLH-related phenotypes to be separated from non-XLH-related phenotypes, such as those noted in *Gy*/Y males. Also, identification of the genetic modifiers of hearing and craniofacial dysmorphology in $Phex^{Hyp\text{-}Duk}$/Y mice could provide insight into the phenotypic variation of XLH in humans.

X-linked dominant hypophosphatemia (XLH) is the most frequently occurring familial form of hypophosphatemic rickets in humans with an incidence of 1 per 20,000 individuals (Burnett et al. 1964; Tenenhouse 1999). XLH is caused by loss-of-function mutations in *PHEX* (phosphate regulating gene with homologies to endopeptidases on the X-chromosome), a gene that encodes an endopeptidase of unknown function (The HYP Consortium 1995). Three X-linked mutations have been identified in the mouse orthologous *Phex* gene: hypophosphatemia, symbolized $Phex^{Hyp}$, hereafter *Hyp* (Eicher et al. 1976); skeletal abnormality 1, symbolized $Phex^{Ska1}$, hereafter *Ska1* (Carpinelli et al. 2002); and gyro, symbolized *Gy* (Lyon et al. 1986). Clinical and biochemical abnormalities observed in *Hyp*/Y, *Ska1*/Y and *Gy*/Y mice and in patients with XLH include renal phosphate wasting, hypophosphatemia, impaired mineralization, and growth retardation.

Correspondence to: E.M. Eicher; eme@jax.org.
*Both authors contributed equally to this research.

The *Hyp* mutation is a spontaneous deletion that begins in exon 15 and extends through exons 16–22 (Strom et al. 1997) into downstream intergenic sequences (Sabbagh et al. 2002). The *Ska1* mutation is a chemically induced point mutation in a splice donor site immediately following exon 8 (Carpinelli et al. 2002). The *Gy* mutation is a radiation-induced deletion that removes 160–190 kb, including exons 1–3 and the *Sms* (spermine synthase) gene (Lorenz et al. 1998; Strom et al. 1997). Given that the gyro deletion includes more than one gene, the previous allelic symbol $Phex^{Gy}$ is inadequate; this mutation is here renamed gyro deletion region, symbol *Gy* (Mouse Genome Database, http://www.informatics.jax.org). Because neither the *Hyp* nor *Gy* mutations is restricted to the *Phex* coding sequence, it has been problematic to assign a specific phenotype solely to the *Phex* gene.

Here we report the identification of two new spontaneous intragenic deletions in the mouse *Phex* gene, hypophosphatemia-2 Jackson, symbolized $Phex^{Hyp\text{-}2J}$ (*Hyp-2J*) and hypophosphatemia-Duke, symbolized, $Phex^{Hyp\text{-}Duk}$ (*Hyp-Duk*). Mice carrying either mutation, together with those carrying *Ska1*, represent valuable animal models for human XLH because each mutation is restricted solely to the *Phex* gene. In addition, the resulting abnormal phenotypes produced by these mutations help clarify the specific contribution of a mutated *Phex* gene to the overall phenotypes observed in *Hyp*/Y and *Gy*/Y mice. Finally, the findings reported here may help define the function of *Phex* in the pathway of bone mineralization and phosphate homeostasis, as well as provide insight into the varying severity noted in humans with XLH.

Materials and methods

Phex alleles

The *Hyp-2J* allele is a spontaneous mutation that occurred in an inbred C57BL/6J mouse at The Jackson Laboratory and is maintained by mating a *Hyp-2J*/+ female to a C57BL/6J +/Y male. The *Hyp-Duk* allele arose at Duke University as a spontaneous mutation in an inbred strain of BALB/cAnBom-$Foxn1^{nu}$, and mice carrying *Hyp-Duk* were imported to The Mouse Mutant Resource at The Jackson Laboratory (Davisson 1990). *Hyp-Duk* is maintained by mating a *Hyp-Duk*/+ female to a +/Y male or a +/+ female to a *Hyp-Duk*/Y male (for simplicity, BALB/cAnBomUrd is shortened to BALB/cUrd). The origins of the *Hyp* and *Gy* mutations have previously been reported (Eicher et al. 1976; Lyon et al. 1976). *Hyp* is maintained by mating a *Hyp*/+ female to a C57BL/6J +/Y male. *Gy* is maintained by mating a *Gy*/+ female to a B6EiC3SnF1-*a/A* +/Y male.

Mice

Mice were housed in polycarbonate cages (51 sq in) on sterilized Northern White Pine shavings bedding and maintained under 14:10 hour light:dark cycles. Acidified water (pH of 2.8–3.2) and sterilized NIH 31 diet (6% fat diet, Ca:P of 1.15:0.85, 19% protein, vitamin and mineral fortified; Purina Mills International) were freely available. All analyses were conducted with mutant males and same-sex littermate controls. (An exception involved craniofacial examinations in which inbred C57BL/6J males were used for comparison with *Hyp-2J*/Y males.) For each experiment, the numbers of mutant and control males are provided in the Results section.

Serum phosphorus and calcium levels

Blood was obtained from the retro-orbital sinus of male mice at 6 weeks of age and allowed to clot on ice for 2–3 h. Serumwas isolated by centrifugation at 7200 g for 10 min and stored at 4°C. Serum phosphorus and calcium levels were determined with the Beckman SYNCHRON CX5 DELTA System (Beckman Coulter, Inc.). To monitor changes in

calibration, along with analytical error and imprecision, Liquid Comprehensive Chemistry Control Serum Levels 1, 2, and 3 were used according to the manufacturer's instructions for Quality Control. The limits of detection for Ca^{2+} and PO_4 are between 2 and 15 mg/dL and 1.0 and 12.0 mg/dL respectively.

PIXImus measurements

Areal Bone Mineral Density (aBMD), % lean body mass, and total body weight were determined on 6-week-old males anesthetized by intraperitoneal injection with Avertin (tribromoethanol stabilized in tertiary amyl hydrate), 1 mg per 2 g of body weight. Measurements were determined by using the PIXI*mus* small animal dual-energy X-ray absorptiometry (DEXA) system (Lunar Corp.), with data analysis by software version 1.46. Areal bone mineral density is a two-dimensional measurement comprised of mineral within the area determined to be bone by the preset thresholds in the PIXI*mus* densitometer. Lean body mass measured by the PIXI*mus* includes both lean mass and body water. The combined value is divided by the total body weight and multiplied by 100 to derive % lean body mass. The resolution of the PIXI*mus*is 0.18 ×0.18mm pixels with a usable scanning field of 80 × 65 mm, allowing for measurement of single whole mice and collections of isolated specimens. Calibrations were performed with a phantom of known density, and quality assurance measurements were performed daily with this same phantom. Assessment of accuracy for the PIXI*mus* was done with a set of hydroxyapatite standards (0–2000 mg), yielding a correlation of 0.999 between standards and PIXI*mus* measurement of mineral. The precision for aBMD is >99% for whole body and ~98.5% for specialized regions.

Whole-body X-ray photography

X-ray films were taken of male mice at 6 weeks of age with a Faxitron MX-20 Specimen Radiography System (Wheeling, Illinois) and Kodak MR 2000-1 film (Eastman-Kodak). Measurements were taken at 23KV at 5×magnitude for 3 s.

Craniofacial measurements

Craniofacial measurements on skulls were determined on male mice at 12 weeks of age. Skull measurement landmark descriptions (Fig. 1) and preparation protocols can be found at The Jackson Laboratory Craniofacial Mutant Resource's website (http://www.jax.org/cranio/characteristics.html).

Histology

Tissues were fixed in anesthetized mice by intracardiac perfusion of Bouin's fixative following a 10 to 20 mL flush with physiological saline. Representative paraffin histological sections of all organs were prepared and stained with hematoxylin and eosin (H&E). Inner ears were dissected, demineralized in Bouin's fixative, serial sectioned, and stained with H&E. To identify precipitate observed in perilymph and endolymph of the inner ear, we stained sections with periodic acid-Schiff (PAS), phosphatungstic acid hematoxylin (PTAH), and von Kossa stains. For gross examination, whole mounts of inner ears were fixed and cleared for examination as described previously (Ward-Bailey et al. 2000).

Auditory brainstem response (ABR) analysis

Hearing was assessed in mutant and control males between 4 and 42 weeks of age by ABR threshold analysis with equipment from Intelligent Hearing Systems with previously described methods and equipment (Zheng et al. 1999). Evoked responses to broadband click and pure-tone 8 kHz, 16 kHz, and 32 kHz auditory stimuli were recorded; however, for clarity of presentation, only click responses are presented. (The three pure-tone auditory stimuli gave similar results.)

RT-PCR analysis

Total RNA was prepared from brain tissue of *Hyp-2J*/Y, *Hyp-Duk*/Y, and respective control mice with Trizol reagent (Life Technologies) as recommended by the manufacturer. First-strand cDNA synthesis was carried out from 1 μg of total RNA with oligo (dT) primer and reverse transcriptase (Amersham Biosciences). As a PCR template, 1–10 ng of first-strand cDNA was used for nested PCR reactions with *Phex*-specific primers. The amplification products were used for direct DNA sequencing.

DNA sequencing

PCR-amplified cDNA was sequenced with a BigDye terminator cycle sequencing kit (Applied Biosystems) and *Phex*-specific primers on an ABI 3100 automated sequencer.

Southern blot analysis

Genomic DNA (~5 μg) from *Hyp-2J*/Y, *Hyp-Duk*/Y, and +/Y littermate controls was extracted from kidney or tail tip, digested with *Hin*dIII, electrophoresed on 0.7% agarose gels, and blotted to Nylon membranes (PALL) by alkaline transfer. Hybridizations were generally performed in a hybridization buffer containing 1.5 × SSPE, 1% SDS and 10% dextran sulfate at 65°C. Probes were labeled by random hexamer priming. Washing was done under stringent conditions (0.1 × SSC, 0.1% SDS at 65°C for 15 min). The mouse genome assembly sequence (http://www.ensemble.org) was used to determine the expected length of the *Hin*dIII restriction fragments containing *Phex* exons 12–18.

Genomic PCR

Primers designed from the mouse genome assembly sequence (http://www.ensemble.org) were used for DNA amplification of all 22 *Phex* exons (Table 3). After an initial denaturation for 5 min at 95°C, amplification cycles consisted of denaturation at 95°C for 30 s, annealing at the exon-specific temperature for 30 s, and 30 s extension at 72°C for 35 cycles, followed by a final extension for 5 min at 72°C. Reaction volumes (25 μL) contained 50 mM KCl, 10 mM Tris-HCl (pH 8.0), 1.5 mM MgCl2, 200 μM of each dNTP, 0.3 μM of each primer, 1 U AmpliTaq Gold polymerase (Applied Biosystems), and 100 ng of genomic mouse DNA.

Statistical analysis

Descriptive statistics are presented as mean ± SEM. All statistical analyses were performed with StatView 4.5 software for Macintosh (Abacus Concepts). Individual genotype means were assessed for significant differences by Fisher's Protected LSD test. Differences were deemed statistically significant when $p \leq 0.05$ unless otherwise noted.

Results

New Phex mutations

The spontaneous X-linked *Hyp-2J* mutation arose at The Jackson Laboratory in 1998 in the C57BL/6J inbred mouse strain. Hemizygous males (*Hyp-2J*/Y) and heterozygous females (*Hyp-2J*/+) resembled *Hyp*/Y males and *Hyp*/+ females, respectively, with shortened hind legs and tail, and a squared trunk. Because *Phex* was an obvious candidate gene for the observed phenotypes noted in *Hyp-2J* mutant mice, its molecular characterization was pursued (see molecular analysis below).

The *Hyp-Duk* mutation arose spontaneously in an inbred BALB/cAnBomUrd-*Foxn1*^{nu} mouse strain at the Department of Urology Research, Duke University. All affected males are mildly growth retarded in overall body size, with a squared shortened body, shortened

hind limbs and tail, and some exhibit circling behavior. In contrast, not all *Hyp-Duk*/+ females show evidence of growth retardation and circling phenotypes, making it difficult to distinguish some heterozygous (*Hyp-Duk*/+) females from normal (+/+) females. For this reason, only *Hyp-Duk*/Y males were chosen for examination. The *Hyp-Duk* mutation was mapped utilizing an F_2 intercross with CAST/Ei to the region of the X Chr containing the *Phex* gene, and serum phosphate analysis indicated that affected males were hypophosphatemic (Table 1). Molecular testing of *Phex* as a candidate gene then was pursued.

Serum chemistry

Serum PO_4 and Ca^{2+} levels were assessed at 6 weeks of age in *Hyp*/Y, *Hyp-2J*/Y, *Hyp-Duk*/Y, *Gy*/Y males and same-sex littermate controls by using the Beckman Synchron CX5 DELTA System (Beckman Coulter, Inc.). All mutant males had serum PO_4 levels (2.95–4.45 mg/dL) significantly lower than controls (Table 1). Statistically significant hypocalcemia also was present in all mutants within the same range (8.38–9.17 mg/dL) (Table 1). The serum PO_4 and Ca^{2+} levels found in *Hyp*/Y and *Gy*/Y mice were consistent with those previously reported (Eicher et al. 1976;Lyon et al. 1986).

Histology

Whole-body histopathological examination was conducted on mutant and control males between 6 and 40 weeks of age. In general, under-mineralized bone was present throughout the body of all mutant males. Growth plates of the knee were thickened and irregular (Fig. 2). A whole-body examination found no obvious lesions in any major organs.

Body composition, bone density, and X-ray analyses

Mutant and littermate control males were analyzed at 6 weeks of age by dual-energy X-ray absorptiometry (DEXA) (PIXI*mus*, Lunar Corp.) for whole-body aBMD and body composition (Table 1). All four types of mutants had significantly lower whole-body aBMD and a trend toward higher lean body mass than wildtype male controls. Differences in lean body mass were significant only in *Gy*/Y and *Hyp-Duk*/Y males when compared with controls. In addition, *Gy*/Y males weighed significantly less than the other three types of mutant males and ~50% less than their wildtype sibling male controls. In contrast, *Hyp*/Y, *Hyp-2J*/Y and *Hyp-Duk*/Y males weighed ~25% less than their male controls. Subsequent to DEXA analysis, an X-ray at 5×magnification was taken of the body by using a Faxitron MX-20 Specimen Radiography System (Faxitron X-ray Corp.). In all mutant males, shortened and thickened long bones with very disorganized femoral growth plates and splayed tibia and fibula were noted, a finding previously reported in *Hyp*/Y and *Gy*/Y mice (Eicher et al. 1976;Lyon et al. 1986).

Craniofacial characterization

Morphological data on skulls were collected from *Hyp-Duk*/Y and *Hyp-2J*/Y males and their respective controls at 12 weeks of age (Table 2). Skulls of *Hyp-2J*/Y mice were significantly shorter in length and width, lower in aBMD, and significantly larger in inner canthal distance than control males. However, skull height, nose length, and lower/upper jaw length were not significantly different.

Comparison of *Hyp-Duk*/Y skulls with +/Y littermate control skulls revealed a reduction in nose, upper jaw, and overall skull length, as well as a reduction in skull aBMD. However, skull width and skull-to-nose length ratio were not different (Table 2).

Auditory brainstem response (ABR) analysis and ear pathology

The average ABR thresholds of *Gy*/Y, *Hyp*/Y and *Hyp-Duk*/Y males were significantly higher than those of +/Y controls, but not for *Hyp-2J*/Y males (Fig. 3). Mean ABR threshold differences between mutants and controls were 48 dB for *Hyp-Duk* (*t*-test $p < 0.0001$), 20 dB for *Hyp* ($p = 0.002$), 21 dB for *Gy* ($p = 0.02$), and 5 dB for *Hyp-2J* ($p = 0.4$). The average ABR thresholds of *Gy*/Y and *Hyp*/Y males were not significantly different from each other ($p = 0.38$), but were slightly higher than those of *Hyp-2J*/Y mice ($p < 0.01$) and much lower than those of *Hyp-Duk*/Y males ($p < 0.0001$).

Because the *Hyp*, *Gy*, *Hyp-2J*, and *Hyp-Duk* mutations cause complete loss of *Phex* function, the more severe hearing loss exhibited by *Hyp-Duk*/Y mice is likely the result of strain background genetic differences. To examine this possibility, a BALB/cUrd *Hyp-Duk*/+ female was mated to a BALBc/ByJ +/+ male. The average ABR thresholds of the mutant male offspring (F_1-*Hyp-Duk*/Y) were 35 dB lower than those of BALB/cUrd *Hyp-Duk*/Y males ($p < 0.001$), but not significantly different from those of *Gy*/Y males ($p = 0.2$) or *Hyp*/Y males ($p = 0.7$) (Fig. 3). These results suggest that homozygosity for recessive factors (genetic modifiers) present in the BALB/cUrd strain exacerbate the hearing loss in *Phex* mutant mice.

ABR tests were performed on *Hyp-Duk*/Y mice at different ages to determine whether hearing loss increases over time (Fig. 4). Regression analysis showed no significant associations of test age with ABR thresholds ($p > 0.3$), indicating that the hearing loss associated with the *Hyp-Duk* mutation is not progressive. Of the 20 *Hyp-Duk*/Y mice tested for ABR thresholds, 11 showed circling behavior indicative of vestibular dysfunction. The 9 non-circling males actually had slightly higher ABR thresholds (mean = 93.8 dB) than the circling males (mean = 79.1 dB SPL; *t*-test $p = 0.04$). Thus, the degree of auditory dysfunction is independent of the degree of vestibular dysfunction in *Hyp-Duk* mutant males.

The whole mounts of inner ears from six *Hyp-Duk*/Y mutant males were compared with three +/Y controls. No gross morphological abnormalities were noted. Examination of cross-sections of mutant cochleas, however, revealed several pathological abnormalities (Fig. 5). The temporal bone surrounding the cochlea was thickened in *Hyp-Duk*/Y males, with many interspersed areas of non-mineralization. A precipitate or infiltrate was usually observed in the scala tympani of the cochleas, but also occasionally in the scala vestibuli. This precipitate stained nonspecific for the stains PAS, PTAH, and von Kossa. Degeneration of the organ of Corti and spiral ganglia was obvious in the apical turn of the cochlea, but the severity of degeneration decreased towards the base. Endolymph volume appeared greater in the cochleas, resulting in an increased scala media and a diminished scala vestibule, with a consequent displacement of Reissner's membrane. Cochlear cross-sections of three *Hyp-2J*/Y males showed thickening of the temporal bone and cochlear precipitates, but no degeneration of the organ of Corti and the spiral ganglion cells.

Molecular analysis of the Hyp-2J mutation

Overlapping RT-PCR products corresponding to *Phex* exons 1–9 and 7–22 were sequenced by using total RNA isolated from two *Hyp-2J*/Y and one +/Y male mice. No DNA sequence variation was found in exons 1–9. Within the amplified transcript comprising exons 7–22, exon 15 was absent.

To confirm that the *Hyp-2J* mutation involves the deletion of exon 15, we performed Southern blot analysis on *Hind*III-digested genomic DNA from mutant and control males. The probe consisted of an RT-PCR product corresponding to *Phex* exons 12–18. A~7.3 kb fragment corresponding to *Phex* exon 15 was deleted in *Hyp-2J*/Y DNA (Fig. 6), whereas

fragments corresponding to *Phex* exon 12 (4.8 kb), exon 13 (6.4 kb), exon 14 (2.8 kb), exon 16 (4.5 kb), and exons 17, 18 (10.8 kb) were present. PCR primers were designed to confirm the deletion of exon 15 in genomic DNA. The combined RT-PCR, genomic PCR, and Southern blot analysis indicated that the *Hyp-2J* deletion involves at least 7.3 kb of DNA containing *Phex* exon 15.

Molecular analysis of the Hyp-Duk mutation

The public mouse genome assembly sequence was used to design intronic primers for the PCR amplification of all 22 *Phex* exons (Table 3). Genomic DNA was isolated from two *Hyp-Duk*/Y and two +/Y male mice. While all exons were amplified in +/Y DNA, *Phex* exons 13 and 14 were missing in *Hyp-Duk*/Y DNA.

To confirm the deletion of the two exons, an RTPCR product corresponding to *Phex* exons 12–18 was hybridized to a Southern blot of genomic DNA. The two *Hin*dIII fragments corresponding to exon 13 (6.4 kb) and exon 14 (2.8 kb) were deleted in *Hyp-Duk*/Y DNA (Fig. 6). Furthermore, instead of the 7.3-kb *Hin*dIII fragment containing *Phex* exon 15 present in +/Y DNA, a 3.8 kb junction fragment was detected in the *Hyp-Duk*/Y DNA. The *Hin*dIII fragments corresponding to *Phex* exon 12 (4.8 kb), exon 16 (4.5 kb), and exons 17, 18 (10.8 kb) were present in mutant and control DNA. In summary, genomic PCR and Southern blot analysis indicated that the *Hyp-Duk* deletion involves at least 30 kb containing *Phex* exons 13 and 14.

Discussion

Male mice hemizygous for the *Phex* mutant alleles *Hyp*, *Hyp-2J*, *Hyp-Duk*, *Gy*, or *Ska1* exhibit similar clinical phenotypes characterized by shortened hind legs and tail, shortened squared trunk, hypophosphatemia due to impaired renal absorption of phosphate, hypocalcemia, and rachitic bone disease. In addition, male mice hemizygous for *Hyp*, *Hyp-2J*, *Hyp-Duk*, or *Gy* mutant alleles have decreased aBMD, which is attributed to the under-mineralization of the skeleton (no aBMD data have been reported for *Ska*/Y males). *Hyp-Duk*/Y males exhibit a circling phenotype similar to that described in the *Gy*/Y males, which is rare in *Hyp*/Y and *Hyp-2J*/Y males and not reported for *Skal*/Y males (Carpinelli et al. 2002).

The original *Hyp* mutation involves a deletion of the *Phex* gene starting in intron 15 and extending through the 3′ region and ~10 kb beyond, but does not include the next downstream gene *Sat* (Sabbagh et al. 2002). We found that the deletion breakpoints for *Hyp-2J* are in introns 14 and 15 of the *Phex* gene and that those for *Hyp-Duk* are in intron 12 and intron 14 (Fig. 7). The deletion of *Phex* exon 15 in the *Hyp-2J* allele and exons 13 and 14 in the *Hyp-Duk* allele lead to a premature stop codon in the open reading frame after 94 nucleotides and 156 nucleotides, respectively. The mutations are likely to cause loss of a functional *Phex* protein. Because *Hyp* and *Hyp-2J* mutations arose and are maintained on the same genetic background (C57BL/6J) and both cause a similar phenotype, it is unlikely that either affects expression of a closely linked gene. This suggestion is strengthened by results reported for the mutation, skeletal abnormality 1, symbolized $Phex^{Ska1}$(*Ska1*). *Ska1* was recovered from a C57BL/6J inbred mouse that was the first generation of a random mutagenesis screen with the chemical mutagen N-ethyl-N-nitrosourea (Carpinelli et al. 2002). The *Ska1* mutation involves a point mutation in a splice donor site immediately following exon 8 of the *Phex* gene and causes skipping of exon 8 in the *Phex* mRNA, creating a null allele. We conclude that *Hyp-2J*, *Hyp-Duk*, and *Ska1* are the first mouse mutations restricted to the *Phex* gene, and males carrying these mutations provide better models for the analysis of the pathophysiology of XLH in humans.

In contrast, the *Gy* mutation deletes the first three *Phex* exons together with the upstream spermine synthase (*Sms*) gene (Lorenz et al. 1998). The compromised fertility of *Gy*/Y males is likely the result of a deletion of *Sms. Gy*/Y mice are smaller at birth than their normal male siblings, a condition that persists throughout life (Table 1) and may be attributed to the deletion of the *Sms* gene rather than the strain background.

Differences in lean body mass were significant only in *Gy*/Y and *Hyp-Duk*/Y males compared with their normal male siblings, possibly because of the circling behavior associated with both mutations. Furthermore, the hearing impairment and circling behavior of *Hyp-Duk*/Y males suggest that the disruption of *Phex* is responsible for the circling behavior in *Gy*/Y mice and not the deletion of a contiguous 5′ gene. There are indications that genetic background impacts the circling phenotype. For example, when the *Hyp* mutation is present on the B6EiC3SnF1-*a/A* background (on which *Gy* has been characterized), a subset of *Hyp*/Y mice circled (Meyer et al. 1995).

Hearing impairment was much greater in *Hyp-Duk*/Y males than in *Hyp*/Y, *Hyp-2J*/Y and *Gy*/Y males (Fig. 3). Because all four mutations appear to cause complete loss of *Phex* function, the more severe hearing loss exhibited by *Hyp-Duk*/Y mice is likely the result of strain background effects. Specific factors (genetic modifiers) present in the BALB/cUrd genome that exacerbate the hearing impairment associated with *Phex* mutations are probably recessive because inter-strain F_1 *Hyp-Duk*/Y males did not show this effect. The hearing impairment caused by the *Phex* mutation in *Hyp-Duk*/Y males is non-progressive, at least by 10 months of age (Fig. 4). At older ages, other genetic factors affecting age-related hearing loss may complicate interpretations (Johnson et al 2000).

Inner ear abnormalities were reported previously for *Gy*/Y and *Hyp*/Y males. Similar to our observations in *Hyp-Duk*/Y males, thickening of the temporal bone with bands of incomplete calcification was reported in inner ears of *Gy*/Y mutants (Sela et al. 1982), and a perilymphatic precipitate was reported in cochleas of *Gy*/Y and *Hyp*/Y mutants (Barkway et al. 1988, 1989). These abnormalities, however, cannot cause the hearing impairment observed in *Hyp-Duk*/Y males because the identical temporal bone pathology and cochlear precipitates were noted in normal-hearing *Hyp-2J*/Y mutants. The most likely cause of hearing impairment in *Hyp-Duk*/Y males is a degeneration of the organ of Corti and spiral ganglion cells (Fig. 5). Although there is variability in severity, this cochlear pathology always was noted in *Hyp-Duk*/Y mutants with impaired hearing, but never in normal-hearing *Hyp- 2J*/Y mutants. The organ of Corti is the sensorineural epithelium present along the length of the cochlear duct, consisting of outer and inner hair cells and supporting cells, and spiral ganglia are the afferent neurons of inner hair cells. This sensorineural degeneration, however, may be a secondary consequence of an increased endolymph volume, as evidenced by an enlarged scala media, reduced scala tympani, and displaced Reissner's membrane.

Similar hearing impairment and inner ear pathologies have been reported in humans with X-linked hypophosphatemia, including a thickening of the petrous temporal bone and cochlear dysfunction (Boneh et al. 1987; Davies et al. 1984; O'Malley et al. 1985, 1988; Weir 1977). Transtympanic electrocochleography results suggest that the cochlear abnormality is endolymphatic hydrops (Davies et al. 1984; O'Malley et al. 1985), which is similar to our observation of increased endolymph volume in hearing-impaired *Hyp-Duk*/Y males. The molecular mechanisms and pathways involving the *Phex* gene that underlie hearing impairment and inner ear pathology await further investigation. The *Hyp-Duk*/Y mouse may provide an opportunity to genetically identify modifier genes that interact with *Phex* mutations to cause cochlear dysfunction.

Skull measurements in*Hyp*/Y mice were reported previously by Gonzalez et al., who found that at 10 weeks of age C57BL/6J *Hyp*/Y and B6EiC3Sn-*a*/*A Hyp*/Y males had significantly decreased skull and nose length compared with controls (Gonzalez et al. 1992). This is consistent with our data for *Hyp-Duk*/Y males, indicating that skull and nose length are significantly shorter than in male controls (Table 2). Skull, but not nose length, also was significantly reduced in *Hyp-2J*/Y males. At 10 weeks of age, B6EiC3Sn-*a*/*A Gy*/Y males had significantly smaller skull, nose, and lower jaw lengths than controls. Upper jaw length was not affected, indicating that reduced skull size is not the result of overall smaller skeleton morphology (Shetty and Meyer 1991). However, we did not find similar lower jaw length reduction in *Hyp-Duk*/Y or *Hyp-2J*/Y mutants. The variability in skull morphology of these four mutants suggests that genetic background affects these craniofacial characteristics.

Craniofacial and dental malformations associated with human XLH include retardation of maxillary and mandibular growth (Tracy and Campbell 1968), bossing of frontal and occipital regions, oxycephaly (Marks et al. 1965), and craniosynostosis (Reilly et al. 1964). The retardation of maxillary and mandibular growth in humans is an example of a craniofacial dysmorphology that can be powerfully modeled by mice. Using Ts65Dn mice, Richtsmeier et al. demonstrated that generally the reduction in nose length, upper jaw length, and/or lower jaw length observed in mice could be considered comparable to human craniofacial phenotypes (Richtsmeier et al. 2000). *Hyp-2J*/Y skulls showed no reduction in lower/upper jaw or nose length, whereas *Hyp-Duk*/Y skulls are smaller in nose, skull and upper jaw length, making *Hyp-Duk*/Y mice better models to study craniofacial abnormalities as a result of XLH in humans.

In their mutational analysis study, Holm et al. found no correlation between the severity of XLH and the type or location of the mutation in the *PHEX* gene in humans (Holm et al. 2001). However, they did suggest that other genes and environmental factors affect the severity of the disease, a hypothesis supported by our results presented here for mutations in the *Phex* gene in mice. Although all four *Phex* mutations examined in our study cause loss of function, changes in genetic background effects (i.e., modifier genes) can alleviate or exacerbate the mutant phenotype. Identification of these genetic modifiers in mice will lend insight into the varying severity of the disease in humans.

In summary, these two new mouse models of human XLH reported here offer outstanding resources for pharmacological investigations. In addition, both may help define the function and role of *Phex* in the pathway of bone mineralization and phosphate homeostasis.

Acknowledgments

We thank Wesley G. Beamer and Tali Shalom-Barak for their careful review of this manuscript, as well as H. Hellebrand, Heping Yu, and Sandra Gray for their technical assistance and contribution to this study. We are indebted to Susan Poulton for originally discovering the Hyp-Duk mutation at The Urology Research Department at Duke University. We also thank Roderick Bronson for pathohistological evaluation and Coleen Marden for colony maintenance. This work was supported by grants from the Deutsche Forschungsgemeinschaft (STR304/2-1), by the National Institutes of Health grants RR01183, CF-DE13078-03, contract DC62108 and by the Cancer Core grant CA34196 from the National Cancer Institute.

References

1. Barkway C, Glenn N, Harvey D, Moorjani P, Palmer A, et al. Hearing impairment associated with hypophosphatemia: the Gyro mutant mouse. Hered Deafness Newslett 1988;1:20–21.
2. Barkway C, Glenn N, Moorjani P, Palmer A, Stabler S, et al. Hearing impairment in two mouse mutants with hypophosphatemia. Hered Deafness Newslett 1989;3:20–21.

3. Boneh A, Reade TM, Scriver CR, Rishikof E. Audiometric evidence for two forms of X-linked hypophosphatemia in humans, apparent counterparts of *Hyp* and *Gy* mutations in mouse. Am J Med Genet 1987;27:997–1003. [PubMed: 3425609]
4. Burnett CH, Dent CE, Harper C, Warland BJ. Vitamin-D resistant rickets. Am J Med 1964;36:222–232. [PubMed: 14124689]
5. Carpinelli MR, Wicks IP, Sims NA, O'Donnell K, Hanzinikolas K, et al. An ethyl-nitrosourea-induced point mutation in *Phex* causes exon skipping, X-linked hypophosphatemia, and rickets. Am J Pathol 2002;161:1925–1933. [PubMed: 12414538]
6. Davies M, Kane R, Valentine J. Impaired hearing in X-linked hypophosphataemic (vitamin-D-resistant) osteomalacia. Ann Intern Med 1984;100:230–232. [PubMed: 6691666]
7. Davisson MT. The Jackson Laboratory mouse mutant resource. Lab Anim 1990;19:23–29.
8. Eicher EM, Southard JL, Scriver CR, Glorieux FH. Hypophosphatemia: mouse model for human familial hypophosphatemic (vitamin D-resistant) rickets. Proc Natl Acad Sci USA 1976;73:4667–4671. [PubMed: 188049]
9. Gonzalez CD, Meyer RA Jr, Iorio RJ. Craniometric measurements of craniofacial malformations in the X-linked hypophosphatemic (*Hyp*) mouse on two different genetic backgrounds: C57BL/6J and B6C3H. Teratology 1992;46:605–613. [PubMed: 1290161]
10. Holm IA, Nelson AE, Robinson BG, Mason RS, Marsh DJ, et al. Mutational analysis and genotype-phenotype correlation of the *PHEX* gene in X-linked hypophosphatemic rickets. J Clin Endocrinol Metab 2001;86:3889–3899. [PubMed: 11502829]
11. Johnson KR, Zheng QY, Erway LC. A major gene affecting age-related hearing loss is common to at least ten inbred strains of mice. Genomics 2000;70:171–180. [PubMed: 11112345]
12. Lorenz B, Francis F, Gempel K, Boddrich A, Josten M, et al. Spermine deficiency in *Gy* mice caused by deletion of the spermine synthase gene. Hum Mol Genet 1998;7:541–547. [PubMed: 9467015]
13. Lyon MF, Scriver CR, Baker LR, Tenenhouse HS, Kronick J, et al. The *Gy* mutation: another cause of X-linked hypophosphatemia in mouse. Proc NatI Acad Sci USA 1986;83:4899–4903.
14. Marks SC, Lindahl RL, Bawden JW. Dental and cephalometric findings in vitamin D resistant rickets. J Dent Child 1965;32:259–265. [PubMed: 5318264]
15. Meyer RA Jr, Meyer MH, Gray RW, Bruns ME. Femoral abnormalities and vitamin D metabolism in X-linked hypophosphatemic (*Hyp* and *Gy*) mice. J Orthop Res 1995;13:30–40. [PubMed: 7853101]
16. O'Malley S, Ramsden RT, Latif A, Kane R, Davies M. Electrocochleographic changes in the hearing loss associated with X-linked hypophosphataemic osteomalacia. Acta Otolaryngol 1985;100:13–18. [PubMed: 4040696]
17. O'Malley SP, Adams JE, Davies M, Ramsden RT. The petrous temporal bone and deafness in X-linked hypophosphataemic osteomalacia. Clin Radiol 1988;39:528–530. [PubMed: 3180671]
18. Reilly B, Leeming J, Fraser M. Craniosynostosis in the rachitic spectrum. J Pediatr 1964;64:396–401. [PubMed: 14130713]
19. Richtsmeier JT, Baxter LL, Reeves RH. Parallels of craniofacial maldevelopment in Down syndrome and Ts65Dn mice. Dev Dyn 2000;217:137–145. [PubMed: 10706138]
20. Sabbagh Y, Gauthier C, Tenenhouse HS. The X chromosome deletion in *HYP* mice extends into the intergenic region but does not include the *SAT* gene downstream from *Phex*. Cytogenet Genome Res 2002;99:344–349. [PubMed: 12900584]
21. Sela J, Bab I, Deol MS. Patterns of matrix vesicle calcification in osteomalacia of Gyro mice. Metab Bone Dis Relat Res 1982;4:129–134. [PubMed: 7144561]
22. Shetty NS, Meyer RA Jr. Craniofacial abnormalities in mice with X-linked hypophosphatemic genes (*Hyp* or *Gy*). Teratology 1991;44:463–472. [PubMed: 1962291]
23. Strom TM, Francis F, Lorenz B, Boddrich A, Econs MJ, et al. Pex gene deletions in Gy and Hyp mice provide mouse models for X-linked hypophosphatemia. Hum Mol Genet 1997;6:165–171. [PubMed: 9063736]
24. Tenenhouse HS. X-linked hypophosphataemia: a homologous disorder in humans and mice. Nephrol Dial Transplant 1999;14:333–341. [PubMed: 10069185]

25. The HYP Consortium. A gene (PEX) with homologies to endopeptidases is mutated in patients with X-linked hypophosphatemic rickets. Nat Genet 1995;11:130–136. [PubMed: 7550339]
26. Tracy WE, Campbell RA. Dentofacial development in children with vitamin D resistant rickets. J Am Dent Assoc 1968;76:1026–1031. [PubMed: 5243735]
27. Ward-Bailey PF, Wood B, Johnson KR, Bronson RT, Donahue LR, et al. Neuromuscular ataxia: a new spontaneous mutation in the mouse. Mamm Genome 2000;11:820–823. [PubMed: 11003693]
28. Weir N. Sensorineural deafness associated with recessive hypophosphataemic rickets. J Laryngol Otol 1977;91:717–722. [PubMed: 894124]
29. Zheng QY, Johnson KR, Erway LC. Assessment of hearing in 80 inbred strains of mice by ABR threshold analyses. Hear Res 1999;130:94–107. [PubMed: 10320101]

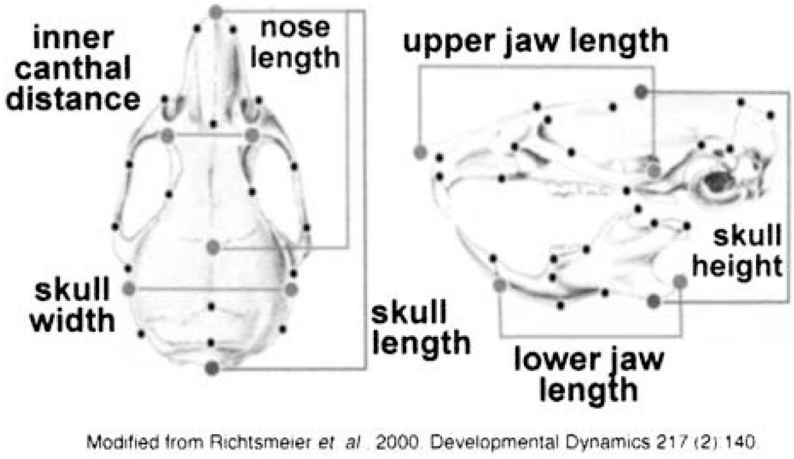

Fig. 1.
Landmarks for craniofacial hand caliper measurements.

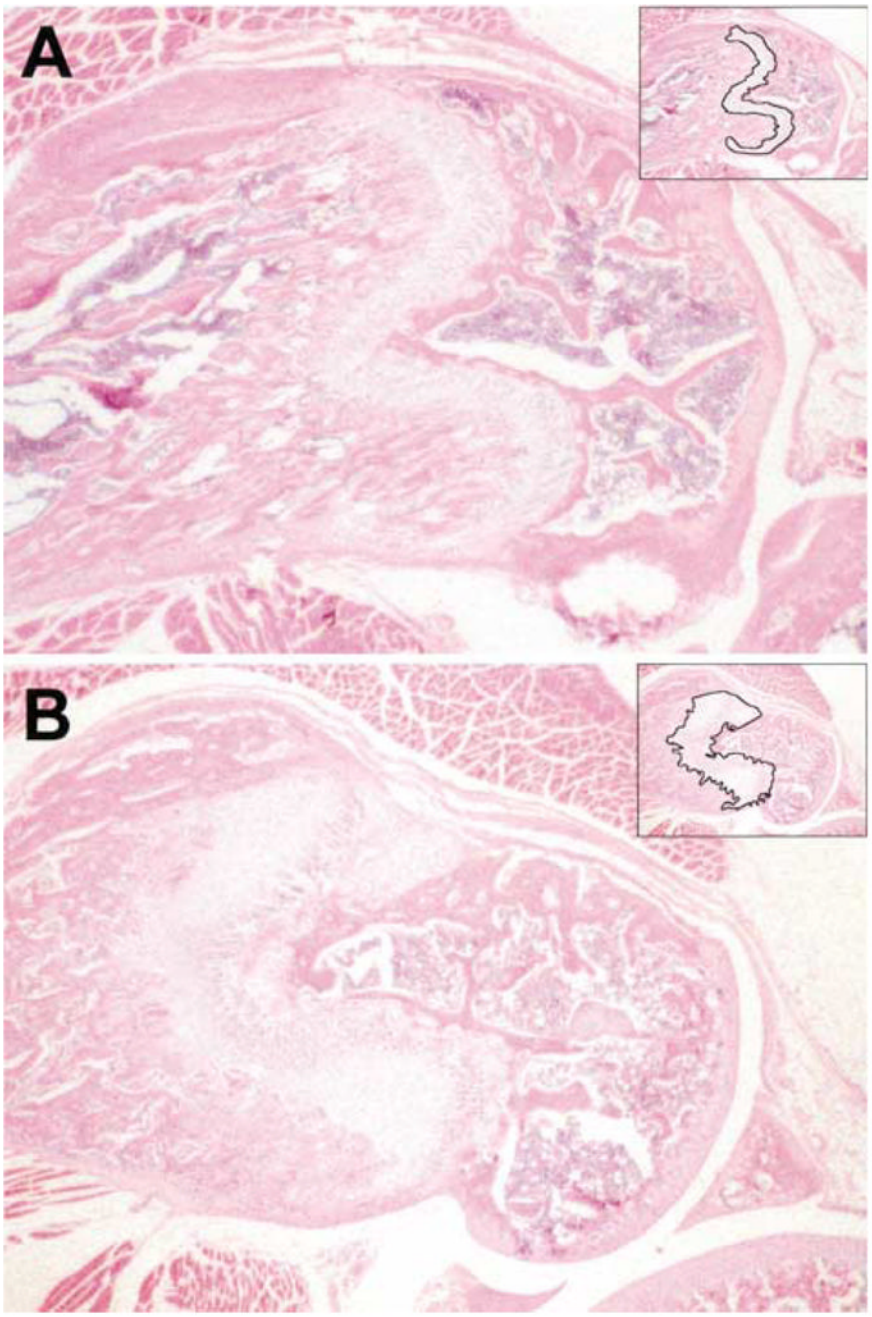

Fig. 2.

Cross-section of the distal femurs of a *Hyp-Duk*/Y mutant male (B) compared with a littermate +/Y control (A) at 6 weeks of age. The growth plate (outlined in the upper right hand corner) of the mutant is thicker than that of the control. The proximal and distal sides of the mutant growth plate are not parallel. Similar pathology was found in *Hyp-2J*/Y mutant males (data not shown).

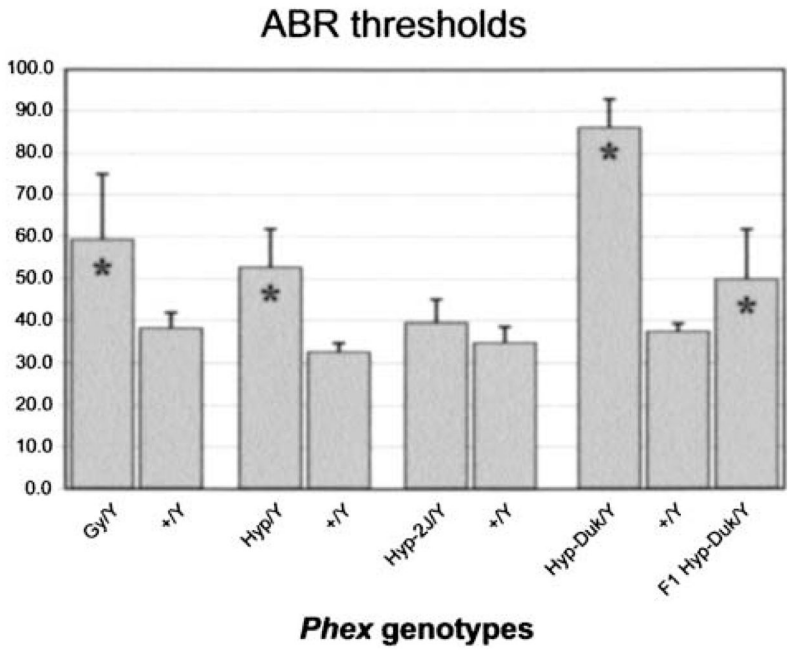

Fig. 3.

Hearing impairment associated with *Phex* mutations. Histogram depicts click ABR threshold means (with bars indicating two standard errors) for (*Gy*/Y; 6 mice, +/Y; 3 mice), (*Hyp*/Y; 4 mice, +/Y; 5 mice), (*Hyp-2J*/Y; 13 mice, +/Y; 5 mice), (*Hyp-Duk*/Y; 20 mice, +/Y; 11 mice), and (BALB/cUrd × BALB/cByJ) F_1-*Hyp-Duk*/Y (F_1-*Hyp-Duk*/Y; 5 mice). Increased values are indicative of hearing impairment (* = $p \leq 0.05$).

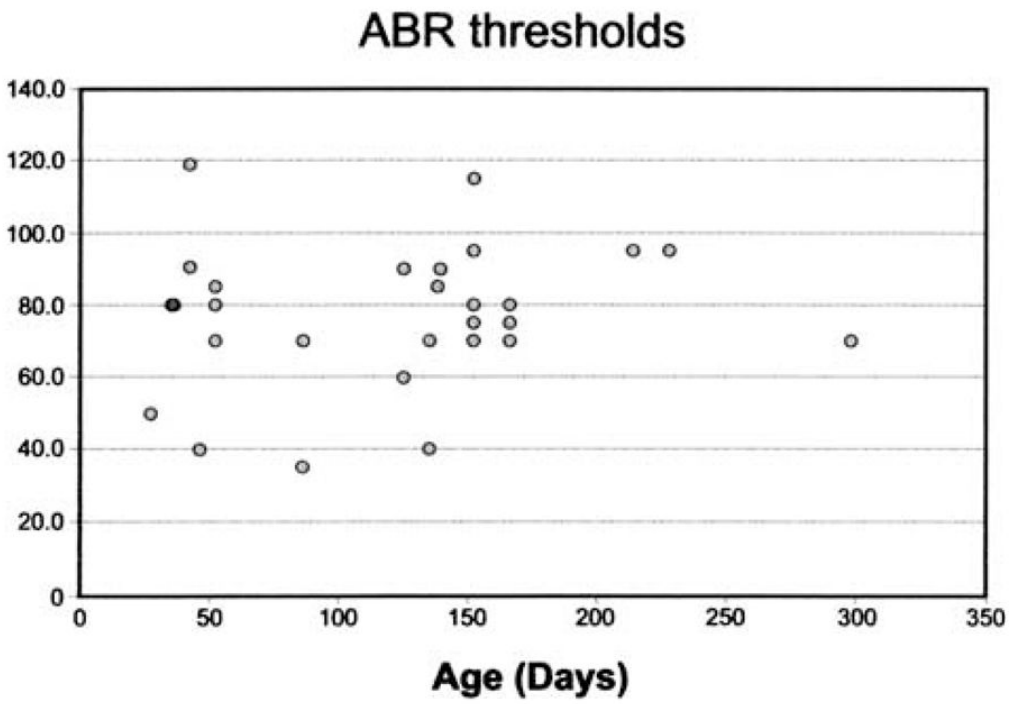

Fig. 4.

Hearing impairment is non-progressive up to 10 months of age. Scatter plot showing ABR thresholds for click stimulus of 20 *Hyp-Duk*/Y mice tested at 32 different ages (range 27–298 days).

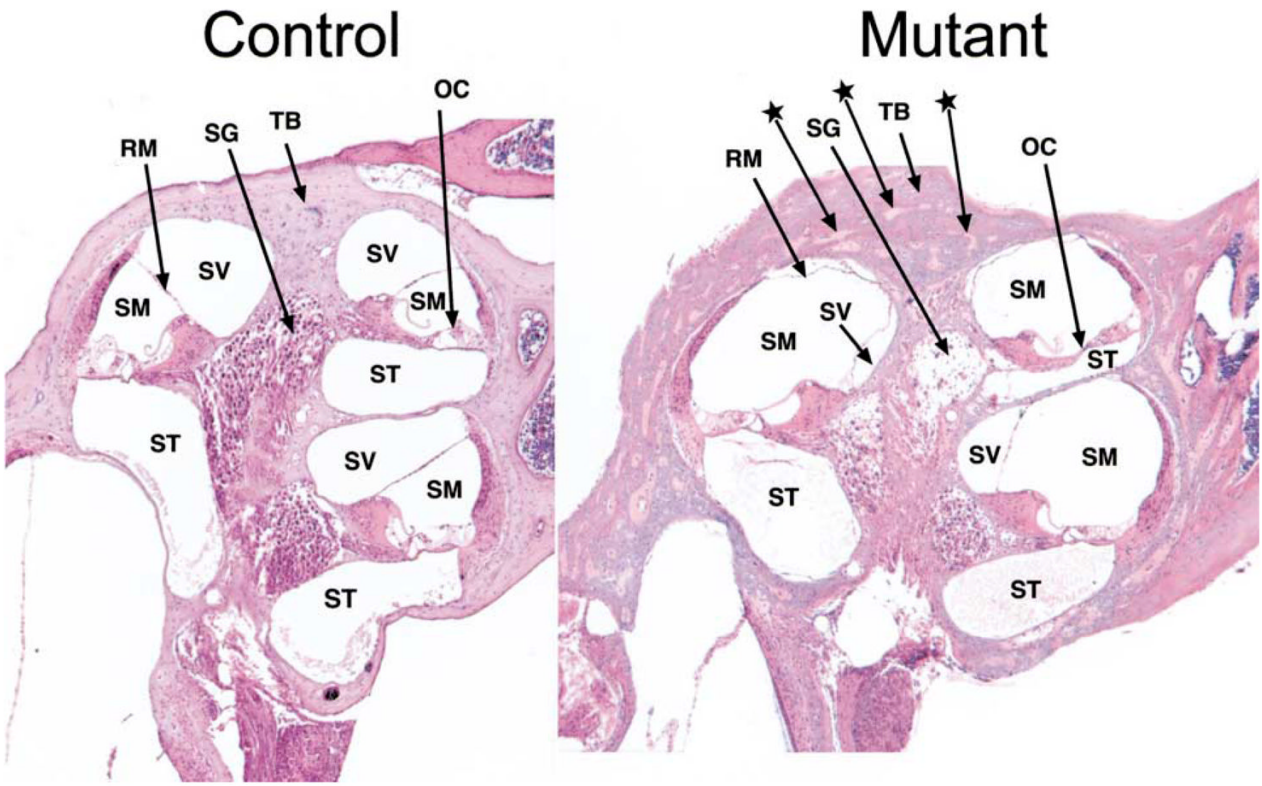

Fig. 5.

Mid-modiolar cross-section through cochleas of a 5-month-old *Hyp-Duk*/Y mutant male (right) compared with an age-matched +/Y control (left). ABR thresholds of the mutant mouse were 50–80 dB above those of the control for all auditory stimuli presented. The temporal bone (TB) surrounding the mutant cochlea is thickened with many areas of nonmineralization (indicated by arrows with stars). A precipitate or infiltrate was often seen in the scala tympani (ST) of mutants. Degeneration of the organ of Corti (OC) and spiral ganglion cells (SG) is apparent in the mutant, especially in the apical turn, as indicated by arrows. Relative to the control, the scala media (SM) of the mutant is increased in size and the scala vestibuli (SV) decreased, with a consequent displacement of Reisner's membrane (RM).

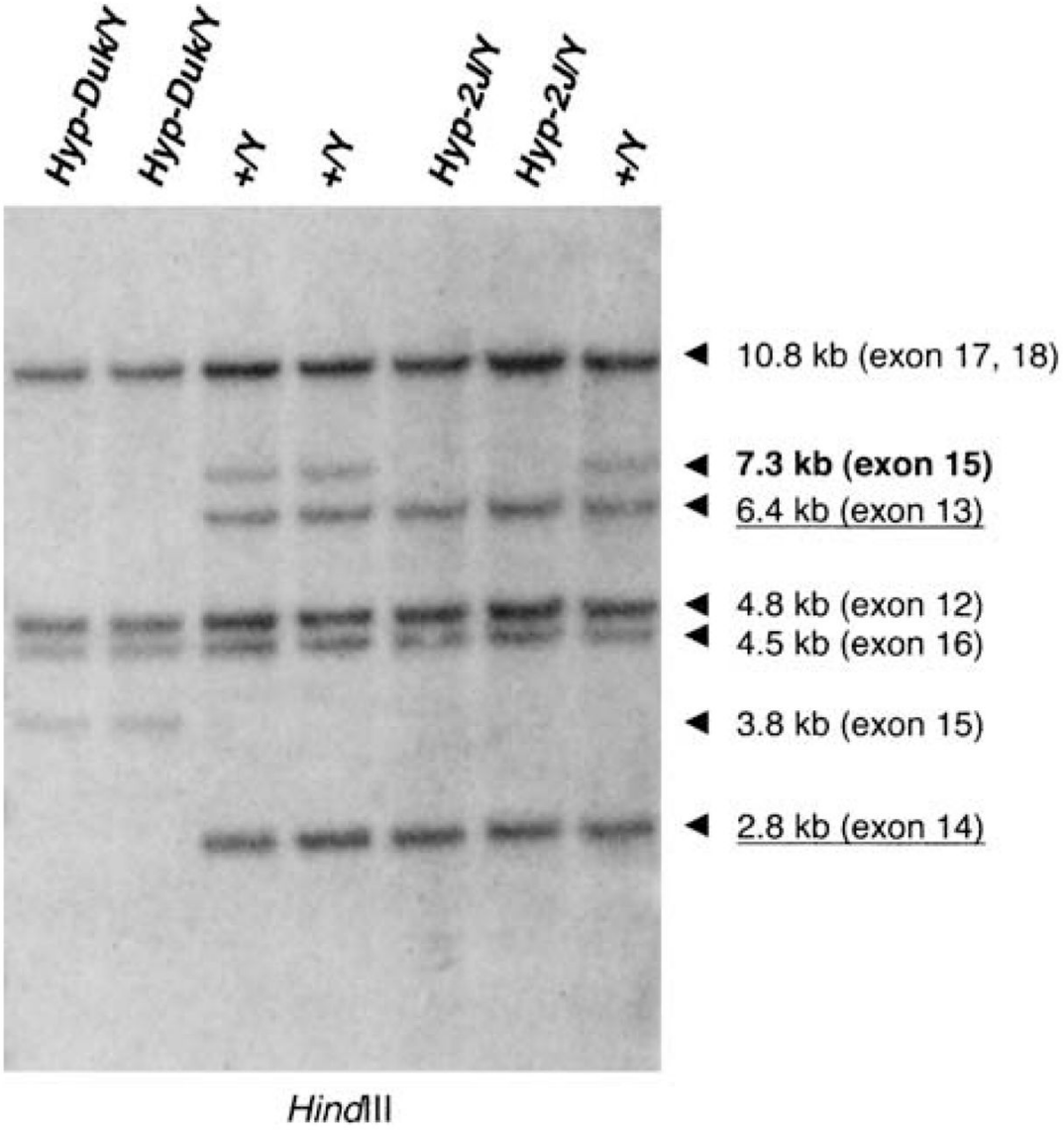

Fig. 6.

Southern blot of *Hin*dIII digests of mouse genomic DNA. Hybridization with an RT-PCR product corresponding to *Phex* exons 12–18. A 6.4-kb fragment corresponding to exon 13 (underlined) and a 2.8-kb fragment corresponding to exon 14 (underlined) were absent in *Hyp-Duk*/Y DNA but present in the control DNA (+/Y). Instead of a 7.3-kb genomic *Hin*dIII fragment containing *Phex* exon 15, a 3.8-kb junction fragment was found in *Hyp-Duk*/Y DNA. In *Hyp-2J*/Y DNA, the 7.3-kb fragment corresponding to *Phex* exon 15 (bold) is absent, while it is present in the control DNA (+/Y).

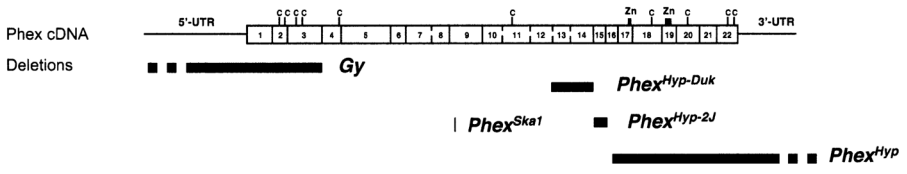

Fig. 7.

Overview of the five mouse *Phex* mutations. The *Gy* mutation deletes the first three *Phex* exons and the complete spermine synthase gene. The *Hyp* mutation deletes the last seven exons and additional undetermined downstream sequence. The *Skal* mutation involves a point mutation in a splice donor site immediately following exon 8 of the *Phex* gene. The *Hyp-Duk* mutation deletes exons 13 and 14, while *Hyp-2J* deletes exon 15.

Table 1

Clinical characterization of *Phex* mutants and controls

Genotype	PO_4 (mg/dL)	Ca^{2+} (mg/dL)	ABMD (g/cm^2)	Weight (g)	% Lean
Hyp-Duk/Y	2.95 ± 0.25*	8.42 ± 0.12*	0.027 ± 3.77E-4*	16.08 ± 0.32*	90.76*
+/Y	9.55 ± 0.22	9.63 ± 0.14	0.037 ± 0.001	20.25 ± 0.42	88.69
Hyp-2J/Y	3.58 ± 0.19*	8.38 ± 0.06*	0.026 ± 2.71E-4*	16.41 ± 0.11*	91.75
+/Y	9.48 ± 0.53	9.80 ± 0.38	0.037 ± 0.001	21.82 ± 0.47	90.89
Hyp/Y	4.45 ± 0.22*	9.15 ± 0.23*	0.025 ± 4.93E-4*	16.85 ± 0.25*	90.98
+/Y	10.47 ± 0.81	10.93 ± 0.68	0.037 ± 0.001	21.89 ± 0.61	90.61
Gy/Y	4.23 ± 0.24*	9.17 ± 0.10*	0.026 ± 0.001*	11.31 ± 1.02*	89.87*
+/Y	8.68 ± 0.37	10.55 ± 0.68	0.039 ± 0.001	25.34 ± 0.88	87.35

All mutants and controls examined at 6 weeks of age.

Data presented are mean ± SEM.

For all values n = 6.

* $p \leq 0.05$.

Mamm Genome. Author manuscript; available in PMC 2010 April 24.

Table 2

Craniofacial characterization of Phex mutants

	Hyp-Duk/Y	+/Y	Hyp-2J/Y	+/Y
Skull				
aBMD (g/cm^2)	0.090 ± 0.003*	0.107 ± 0.002	0.085 ± 0.001*	0.105 ± 0.001[a]
Height (mm)	9.69 ± 0.05	9.48 ± 0.12	9.82 ± 0.11	10.34 ± 0.27
Width (mm)	10.45 ± 0.08	10.37 ± 0.09	10.48 ± 0.15*	11.12 ± 0.22
Length (mm)	21.48 ± 0.31*	22.63 ± 0.14	21.86 ± 0.10*	22.91 ± 0.22
Nose				
Length (mm)	14.12 ± 0.29*	15.09 ± 0.09	14.99 ± 0.16	15.34 ± 0.15
Skull/nose length ratio	1.52 ± 0.02	1.50 ± 0.01	1.46 ± 0.01*	1.49 ± 0.01
Inner canthal distance (mm)	3.79 ± 0.07	3.69 ± 0.07	5.05 ± 0.09*	4.20 ± 0.04
Jaw length				
Lower (mm)	10.86 ± 0.16	10.73 ± 0.17	10.99 ± 0.11	11.13 ± 0.28
Upper (mm)	14.62 ± 0.19*	15.41 ± 0.13	15.67 ± 0.28	15.40 ± 0.24
Jaw length ratio	1.35 ± 0.02*	1.43 ± 0.01	1.43 ± 0.03	0.39 ± 0.02

Mutants and controls were examined at 12 weeks of age.

Data presented are mean ± SEM.

For all values n = 6 unless otherwise noted ([a]n = 10).

*$p \leq 0.05$.

Table 3

Primers used for amplification of *Phex* exons 1–22

Exon	Primer forward	Primer reverse	bp	°C
1	5′-AGAGTCTTGAATATCAAACGCC-3′	5′-AAGAGTCTCCAGAGATGCCC-3′	260	62
2	5′-AACTGTCTTGCGTATGTGCC-3′	5′-TTTGGTCAACCTCAAGCAAAC-3′	266	60
3	5′-TCTTGTCAAACAGTGTTCTGG-3′	5′-CCAGGGAGACATTTGAGGAG-3′	300	60
4	5′-TTTTCTGGAGGCTGACCTTC-3′	5′-TTCTATTGCCCAAACAACACC-3′	296	60
5	5′-AGCTTGGTGAACGAGTTTGG-3′	5′-CATGTGTGACATCCTAAATAGC-3′	506	60
6	5′-TGGAGTGAACTTATTTCTTGGG-3′	5′-ACCAAACAGTAGCCAGACAAG-3′	258	60
7	5′-TCCTTCCTACCAGGCTGTTG-3′	5′-TTGGATACAAAGGGCAATGGC-3′	304	62
8	5′-CATGTGAAAGGCAGTCATGC-3′	5′-AGGCCAAATTTTATACACAGATG-3′	240	60
9	5′-CAGAATGGATTATGCTCGGC-3′	5′-TTTCAAAGCAATTTTCACCGTAC-3′	333	60
10	5′-TTGCCAACAGTTTTCCAAAGG-3′	5′-AAGCTCCCTACATCCCATCC-3′	293	60
11	5′-GACTGGTGTGGGATGGAATC-3′	5′-TCTTGTCTGTCAGATCTGCC-3′	280	60
12	5′-TTCAGGTCAAGGAAACCTGG-3′	5′-AGCACACACCTACCTCTGGG-3′	309	60
13	5′-GAAGACTGAAGCCCTATATCC-3′	5′-TTAGTTAATAGGCATCAGGCC-3′	230	60
14	5′-ATAGCGTCTCTTCTGGTTGC-3′	5′-GCTGGCTACCCTGAGTTGAG-3′	308	60
15	5′-AGTCTTGCCAAACTGTGCTC-3′	5′-GTCACTTACATTGAAAACACTC-3′	387	60
16	5′-TTGGGCTATAGTTGGAACCAG-3′	5′-AGATATTCTGTCCTTGGCCG-3′	217	60
17	5′-AAGGATTATGCTGTCAGATTCATATC-3′	5′-ACAATTAACACCATACAATCAAC-3′	197	60
18	5′-TGTGGGAGCTAATCTCAGGG-3′	5′-GAAGAAAAATGGCCCACAAGG-3′	329	62
19	5′-GCTTGGGCTAGTTTGCTATCTC-3′	5′-TGAGTTGGTGCTATACACGGAG-3′	304	62
20	5′-ACCCATGGCAGGAATATGTG-3′	5′-TGCCAGTGAGTTTTTCCTCC-3′	294	60
21	5′-CCAAAATTGTTCTTCAGTACACC-3′	5′-ATCTGGCAGCACACTGGTATG-3′	258	64
22	5′-TTTGTAGTGGAGTATTTCATCC-3′	5′-AGGCAGAAAGCAGTAGGTGC-3′	324	60